

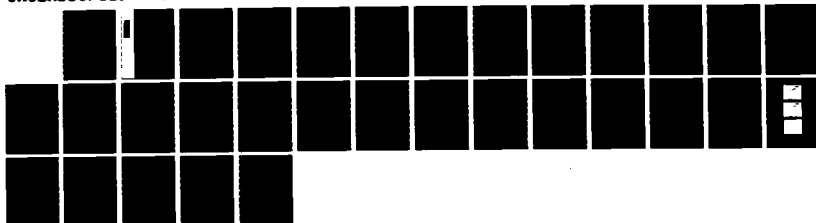
NO-A176 444

DESIGN AND PERFORMANCE OF A THREE-CAVITY GYROKLYSTRON
AMPLIFIER(U) HISSION RESEARCH CORP ALEXANDRIA VA
W H BOLLEN ET AL. APR 86 HRC/MDC-R-111 NRL-MR-5740
N00014-83-C-2192 F/G 9/1

1/1

UNCLASSIFIED

NL





1.0



1.1



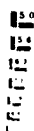
1.25



1.4



1.6



1.8



2.0



2.2



2.5



2.8



3.15



3.5



4.0



4.5

NRL-MR-5740

MRC/WDC-R-111

AD-A176 444

DESIGN AND PERFORMANCE OF A THREE-CAVITY GYROKLYSTRON AMPLIFIER

W. M. Bollen
A. H. McCurdy*
B. Arfin**
R. K. Parker***
A. K. Ganguly***

April 1986

Prepared for: NRL Contract No. N00014-83-C-2192

MISSION RESEARCH CORPORATION
5503 Cherokee Avenue
Alexandria, Virginia 22312

Applied Physics Section*
Yale University
New Haven, CT 06520

Litton, Ind.**
San Carlos, CA 94070

Naval Research Laboratory***
Washington, DC

DTIC FILE COPY

DTIC

ELECTRONICS

FEB 2 1987

This document is the property of the Government and is loaned to you for your use only. It is not to be distributed outside your organization.

Copy 8

DESIGN AND PERFORMANCE OF A THREE-CAVITY GYROKLYSTRON AMPLIFIER

W. M. Bollen
A. H. McCurdy*
B. Arfin**
R. K. Parker***
A. K. Ganguly***

April 1986

Prepared for: NRL Contract No. N00014-83-C-2192

MISSION RESEARCH CORPORATION
5503 Cherokee Avenue
Alexandria, Virginia 22312

Applied Physics Section*
Yale University
New Haven, CT 06520

Litton, Ind.**
San Carlos, CA 94070

Naval Research Laboratory***
Washington, DC

CONTENTS

<u>Section</u>	<u>Page</u>
1 INTRODUCTION	1
2 PREVIOUS WORK	4
3 NRL GYROKLYSTRON DESIGN	7
4 GYROKLYSTRON PERFORMANCE	10
5 CONCLUSIONS	23
6 ACKNOWLEDGEMENTS	24
7 REFERENCES	25



✓
Letter in file
RECEIVED
JAN 11 1964
A-1

LIST OF FIGURES

<u>Figure</u>		<u>Page</u>
1	NRL Gyroklystron Amplifier.	2
2	Schematic of the Gyroklystron Experiment Depicting the Microwave Components.	11
3	Showing the Small Signal Gain.	12
4	Drive Curve.	13
5	Theoretical Bandwidth Curve.	15
6	Experimental Measurements of Output Bandwidth.	16
7	GKA Line Width.	17
8	Theoretical Drive Curve for a Two-Cavity, Phase-Locked Gyroklystron Amplifier.	19
9	Experimental Drive Curve for GKLY-101 Phase-Locked Oscillator Operation.	20
10	Phase-Locked Oscillator Performance.	22

SECTION 1

INTRODUCTION

Millimeter-wave power production using fast-wave amplifiers has shown a large amount of experimental progress in the last decade. Recent studies have focused on the gyroklystron amplifier (GKA) and the gyro-traveling wave tube (gyro-TWT). These devices eliminate the conventional slow-wave circuit by using the periodic motion of the electrons, induced by external fields applied in the interaction region, to couple (synchronize) a natural beam resonance to a selected waveguide mode. With the gyro-devices, an axial magnetic field is used to couple the fast cyclotron wave on the beam to an appropriate transverse electric (TE) waveguide mode. The fast-wave amplifiers are able to generate increased millimeter wave power levels, since their coupling mechanism does not require the small transverse dimensions of the slow-wave circuit; indeed, simple structures such as large scale cavities or lengths of waveguide can be used for gyro-devices.

The Naval Research Laboratory is presently pursuing a program to investigate the performance of gyroklystron devices. The main emphasis is on amplifiers; however, locked-oscillator performance is also being studied. Initial studies have examined a rectangular three-cavity configuration operating at the fundamental frequency and in the dominant cavity mode. The program plan includes future examination of circular cavity devices and device operation in overmoded cavities. The latter approach allows device operation at larger output power levels. The NRL program includes both an experimental^{1,2} and a theoretical^{3,4} effort.

The gyroklystron is of particular interest for radar and advanced accelerator applications, because it should be an efficient (>40%), high gain (>40dB) amplifier capable of generating high-power millimeter waves. The limited bandwidth (>5%) should not adversely affect these applications. The gyroklystron shown in Figure 1 illustrates typical characteristics of a fast-wave device. A magnetron injection gun is used to launch an annular electron beam into the rf interaction region. In Figure 1, the interaction

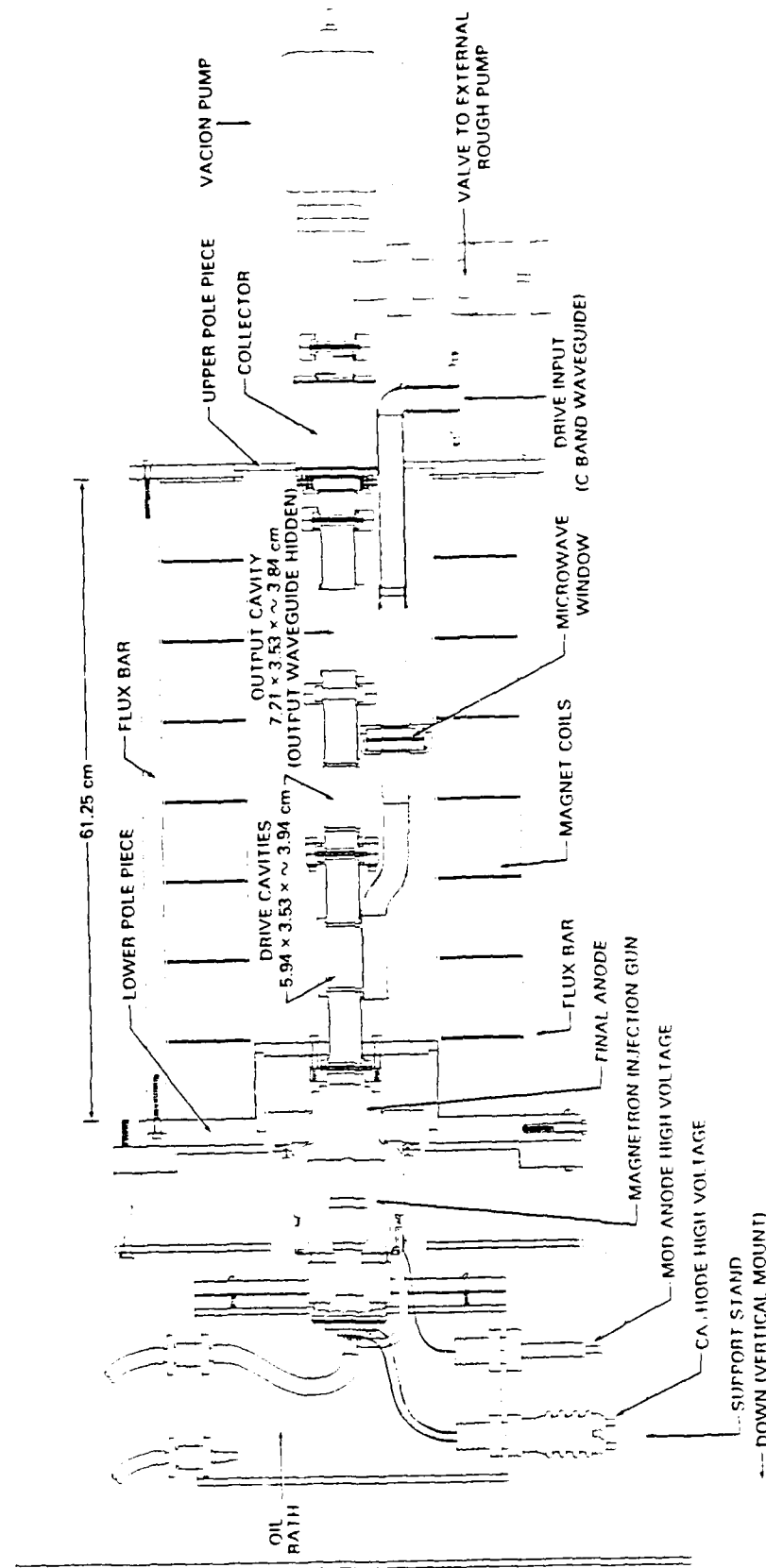


Figure 1: HRL Gyrokystron Amplifier. Shown is a drawing of the HRL gyrokystron amplifier. Only the input waveguide is shown. The other two cavity waveguides are rotated out of the plane of the drawing.

region consists of two drive cavities and one output cavity, with these cavities separated from one another by radiation-free drift spaces. In the cavity regions, the transverse kinetic energy of the electrons is coupled to a selected TE cavity mode by the electron cyclotron resonance condition, where the energy dependence of the relativistic electron cyclotron frequency causes the electrons to become phase-bunched in their cyclotron orbits, thereby giving rise to a coherent interaction. To achieve positive gain, the interaction requires that the radiation frequency slightly exceed the cyclotron frequency. For operation at the fundamental cyclotron frequency, this condition leads to a requirement for a high axial magnetic field in the interaction region. For example, a 35 GHz amplifier would need a magnetic field of approximately 13 kG; our device which operates at 4.5 GHz requires about 2 kG. Since the gyro-devices extract energy from the transverse or rotational motion of the electrons, a large ratio of the transverse to axial electron velocity, α , is required to obtain high efficiency operation. Typical values of α range from 1 to 3.

SECTION 2

PREVIOUS WORK

A good overview of previous gyroklystron amplifier research may be found in articles by Symons,⁵ Jory,⁶ and Andronov.⁷ Table 1 summarizes previous GKA experiments. As Table 1 shows, few actual experiments have been performed to test the gyroklystron amplifier concept, although gyroklystron experiments were begun 20 years ago by Wachtel and Hirshfield.⁸

As shown in Table 1, a two-cavity, 28 GHz gyroklystron amplifier was constructed by Jory.⁹ This device operated at the fundamental cyclotron frequency. It had a circular TE_{011} driver cavity and a circular TE_{021} output cavity. The device never performed to design expectations because of problems with spurious oscillations in the driver cavity and in the drift tubes. However, use of resistive loading did eventually result in stable operation. A gain of 40 dB was reported with an output power of 50 kW.

A three-cavity gyroklystron, operating at the second harmonic of the cyclotron frequency, was also reported by Jory.^{10, 11} Again, competing oscillations hampered operation. The largest output power reported was 20kW, with an 8.2% efficiency.¹⁰ Only a 10 dB gain was realized.

A pre-1967 gyroklystron amplifier was reported by Andronov.⁷ A 70% perpendicular efficiency at X-band with CW operation was reported. Details were not given.

The cyclotron resonance condition is the same for gyroklystrons as for other gyro-devices. Thus, much of the extensive gyromonotron theory⁵ is applicable to the gyroklystron. There are, however, differences, and a body of knowledge related specifically to gyroklystrons has been developed over the years. The earliest work which specifically addresses gyroklystrons is that of Demidovich.¹² He calculated the perpendicular efficiency (the efficiency with which energy is extracted from the rotational motion of the electrons) for a three-cavity gyroklystron to be 85%.

TABLE 1

GYROKLYSTRON DEVICES

	<u>RUSSIAN</u>	<u>VARIAN</u>	<u>VARIAN</u>	<u>NRL</u>
FREQUENCY	X-BAND	28 GHz	10 GHz	4.5 GHz
CYCLOTRON HARMONIC	?	FUNDAMENTAL	SECOND HARMONIC	FUNDAMENTAL
OUTPUT POWER	~2 kW	50 kW	20.6 kW	54 kW
GAIN	?	40 dB	10 dB	30 dB
EFFICIENCY	70% (PERP)	10%	8.2%	30%
BANDWIDTH	?	0.2%	?	0.42 %
BEAM VOLTAGE	?	80 kV	50 kV	35 kV
BEAM CURRENT	?	8 A	5 A	5-10 A
MAGNETIC FIELD	?	11 kG	1.96 kG	1.6 kG
CAVITIES	?	TE ₀₁₁ ⁰ /TE ₀₂₁ ⁰	THREE	TE ₁₀₁ ⁰ /TE ₁₀₁ ⁰ /TE ₁₀₁ ⁰
COMMENTS	CW	SPURIOUS OSC.	SPURIOUS OSC.	

Later, Kolosov¹³ and Kurayev¹⁴ examined the issue of optimum shape for the output cavity of a gyroklystron. They reported perpendicular efficiencies as large as 97%. Total efficiencies (microwave energy divided by beam energy) of 65% have been calculated by Kanavets¹⁵ for a three-cavity relativistic gyroklystron.

Symons¹⁶ has analyzed the GKA in the small signal regime. This theory was used in conjunction with a computer simulation¹⁷ to design the 28 GHz, two-cavity gyroklystron tube in Table 1. An estimate was made of the space-charge effects. Kovalev¹⁸ has also examined space-charge effects. His results show that space-charge effects enhance the growth of electron bunches in the drift tubes, but also increase the velocity spread of the electrons, decreasing the maximum efficiency. Kurayev¹⁹ found similar results.

Keier^{20, 21} has examined the use of nonuniform magnetic fields to optimize the efficiency. He examined the possibility of adjusting the phase-bunching of a gyroklystron beam, with large velocity spread, to optimize the efficiency.

Ganguly³ has examined the theory for a two-cavity gyroklystron. He has shown that use of a circular TE_{011} mode-bunching (driver) cavity with a TE_{041} mode output cavity stabilizes the output cavity to mode competition. He also suggested tapering the magnetic field to increase the efficiency, as is done with gyromonotrons. Recently, Ganguly⁴ has developed a multi-cavity small-signal analysis for gyroklystron amplifiers which we have used to compare with our experimental results.

SECTION 3

NRL GYROKLYSTRON DESIGN

A number of criteria were used in the design of the GKLY-101 gyroklystron amplifier shown in Figure 1. First, due to previous experimenters' difficulties with spurious oscillations, the design was restricted to the fundamental cyclotron frequency operating in the dominant cavity mode. Further, the drift lengths were designed to be cut off to the operating frequency. Second, due to the availability of a particular electron gun, the design was constrained in magnetic field and, therefore, frequency. Thirdly, TE_{101} rectangular cavities were chosen to allow easy tuning and to eliminate the dual polarization possible with a circular TE_{111} cavity. Fourthly, a 40 dB gain was desired; theory showed a three-cavity design would be capable of obtaining this gain.¹ Finally, a decision to use only conventional magnets was made. This was consistent with the other frequency limitation, but, in addition, allowed for greater experimental flexibility (e.g., easy tapering of the magnet field profile). Using these criteria, the GKLY-101 amplifier was designed, fabricated, and is now under test.

As shown in Figure 1, the GKLY-101 tube utilizes a magnetron injection gun to launch an annular electron beam into the rf interaction region, which consists of three cavities separated by radiation-free drift lengths. This gun uses an intermediate electrode to optimize α and operates with temperature limited electron emission to minimize axial velocity spread. The gun was originally designed to provide a 5 A beam with an α of 2 when operating at 60 kV. This is the same gun used in the 10 GHz Varian experiments¹⁰ in Table 1. Preliminary testing has not exceeded 35 kV due to modulator limitations. At this voltage, the α has been determined to be approximately one. This value is based on both experiments and computer simulation of the gun.

The rf circuit consists of three rectangular cavities in series operating in the TE_{101} mode at the fundamental cyclotron frequency. These cavities are separated by cylindrical drift lengths ($L = 1.5 \lambda$, where λ is the free space wavelength) which are cut off to the operating frequency. The

cavities are tunable from 4.4 GHz to 4.5 GHz by moving a foil membrane which forms one of the cavity walls. The cavities were cold tested to assure no unwanted mode competition with the desired mode. The first two cavities ($L = 0.9 \lambda$) are used to bunch the beam and have a cold loaded Q of 600. The third cavity ($L = 1.1 \lambda$) has a cold loaded Q of 235. All three cavities are coupled to waveguides through a hole in the side wall. This permits the drive signal to be introduced into the first cavity and the output hole microwave power to be extracted from the third cavity. The waveguide on the second cavity can be used as a diagnostic for three-cavity operation or to monitor two-cavity gyroklystron operation. All cavities were coupled to the waveguide by positioning a short at the end of the waveguide at approximately $\lambda/4$ from the center of the coupling hole. The optimum position of the short was determined for the center frequency of operation in cold test, and the short was then brazed in this position during fabrication of the tube.

Competing cavity modes near the operation frequency were removed by careful cavity design. However, a mode related to the coupling hole between the cavity and the waveguide was discovered in cold test. This mode was finally removed by altering the coupling hole shape. As a result, the driver cavities have 0.75 inch circular coupling holes, and the output cavity has a 1 inch square coupling hole. The large coupling holes were required to obtain the desired loaded Q values suggested by theory.¹

During hot test, matching circuits (e.g., E-H tuners) have been tried to improve the hot coupling. Matching circuits on both the input and output increased output power at most by 10%, while limiting the output bandwidth of the GKA. For normal operation, without external matching circuits on the input, approximately 10-20% of the drive signal is reflected. This reflection is related to the hot operation of the device and is difficult to improve, because the match changes during the electron beam pulse. Some improvement can be obtained using a sliding short on the input; however, the input bandwidth is then limited. Such a matching circuit was not normally used. For the purposes of our experiment, the match was deemed acceptable; however, for a production device, a better coupling will be required.

The magnetic field for the gyrokystron is supplied by eight conventional magnets in a stack. Iron flux bars and two pole pieces are used to confine the magnetic field. The magnet stack is powered by four supplies, with two adjacent magnets in series to give four modules. This allows tapered magnetic field operation. A ninth magnet, powered by a separate supply, powers the magnetic field for the gun region. The gun resides below the lower iron pole piece. The magnet stack is capable of 2 kG operation, and is adjusted to excite the fundamental cyclotron maser frequency ($B \approx 1.65$ kG).

SECTION 4

GYROKLYSTRON PERFORMANCE

For the performance testing of the GKLY-101 amplifier, the device was operated at a pulse repetition frequency of 60 Hz and a pulse duration of 1 to 3 microseconds. Figure 2 shows schematically how the microwave characteristics were measured. Isolators were used to separate each microwave source in the amplifier chain. Input power, output power, and gain were measured using calibrated directional couplers and thermistor-mount power meters. Diode crystals allowed the microwave pulse shape to be monitored. In a similar manner, a directional coupler was used to monitor the reverse microwave power. The output power was also measured using a calorimetric water load specifically built for the experiment. Efficiency is calculated as the ratio of output microwave power to input beam power. The collector of the tube is isolated allowing the current to be easily measured using a Rogowski monitor on the wire connecting the collector to ground. A capacitive voltage monitor on the gun voltage is used to determine the beam voltage.

Initial tube testing has examined gain, output power and efficiency. Figure 3 shows typical small signal data with a gain of 26 dB. In the figure, V_1 refers to the beam voltage, and V_2 refers to the mod anode voltage. This data is taken with no tapering of the magnetic field and compares well with theoretical predictions of 26 dB small signal gain,⁴ for $\alpha \approx 1$, $\Delta V_2/V_2 < 10\%$, with $\omega/\omega_c = 1.035$ (estimated beam parameters for the experiment), where $\omega_c = eB/m_0c$, B is the axial magnetic field and the other constants are as normally defined. Larger small signal gains (≈ 36 dB) have been observed with a tapered magnetic field.

The largest output power is shown in Figure 4, 54 kW, and was obtained using a tapered magnetic field. The large signal gain was 18 dB, the small signal gain was 22 dB, and the efficiency was 25%. Both the small signal gain and the efficiency are lower than the best values observed (36 dB, 33%). The reason for this is believed to be related to the operation of the gun. The high power is obtained by increasing the current. This probably increases the

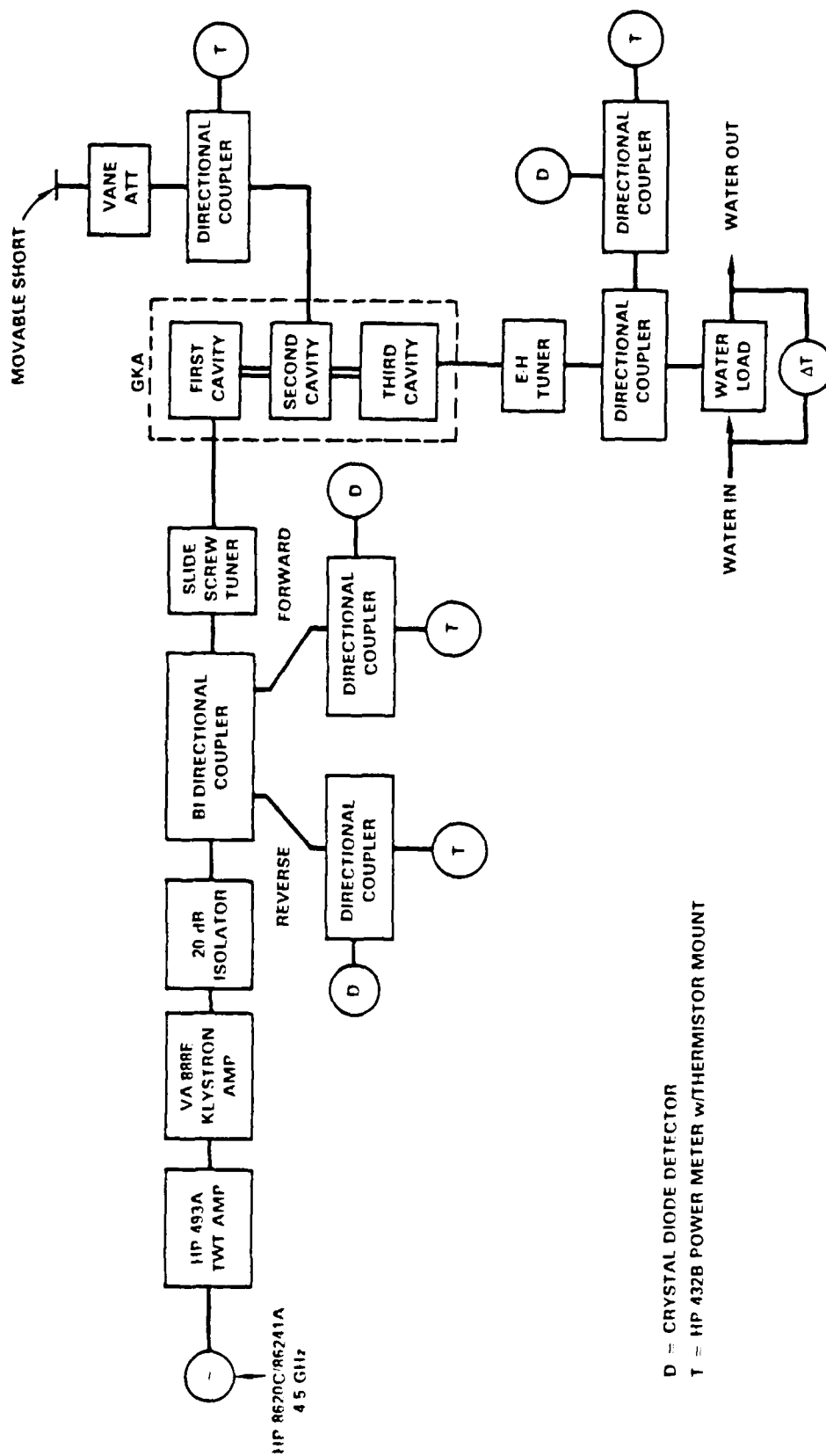


Figure 2: Schematic of the Gyrokystron Experiment Depicting the Microwave Components. (Note, the slide tuner was normally not used.)

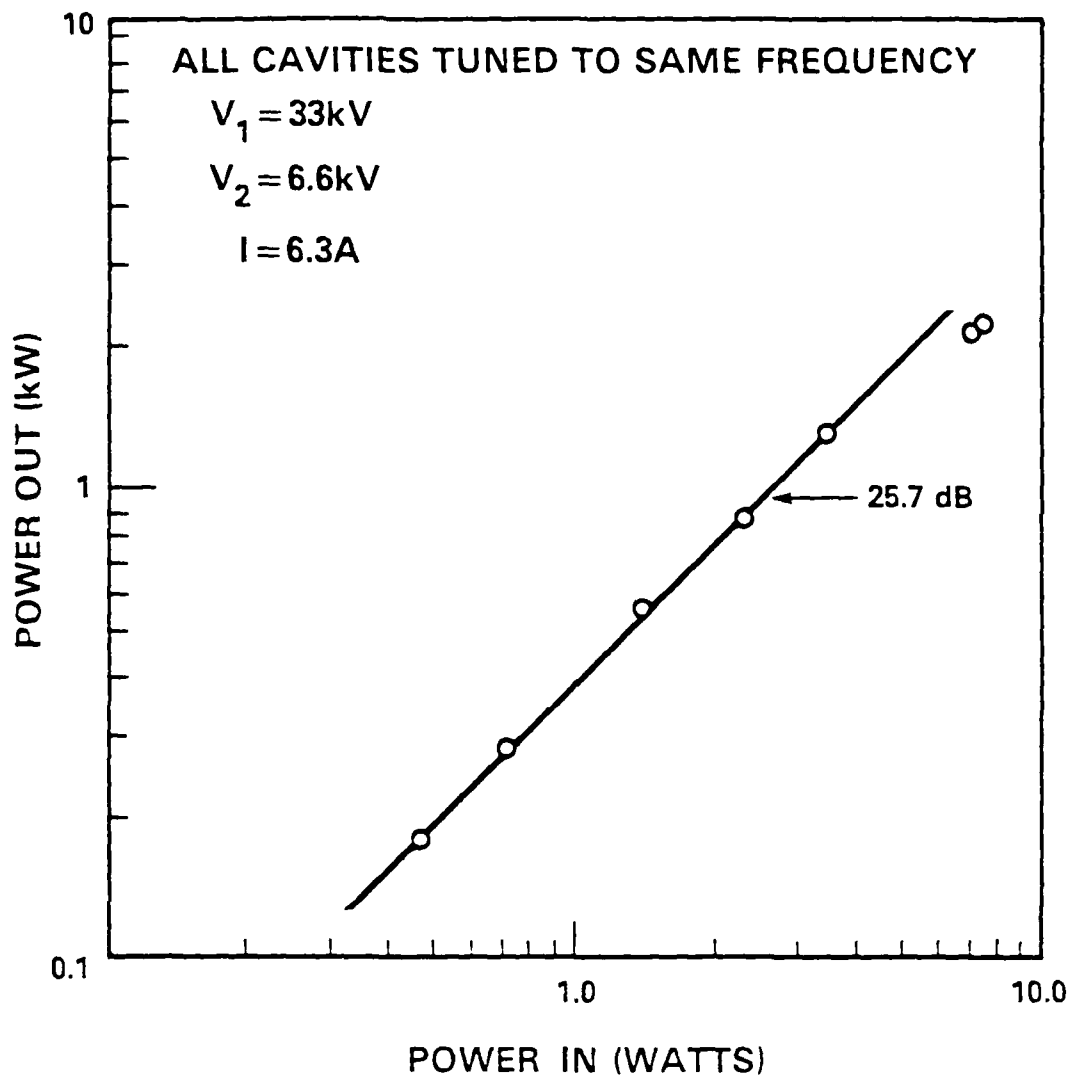


Figure 3. Small Signal Gain. Experimental drive curve in a uniform magnetic field showing the small signal gain.

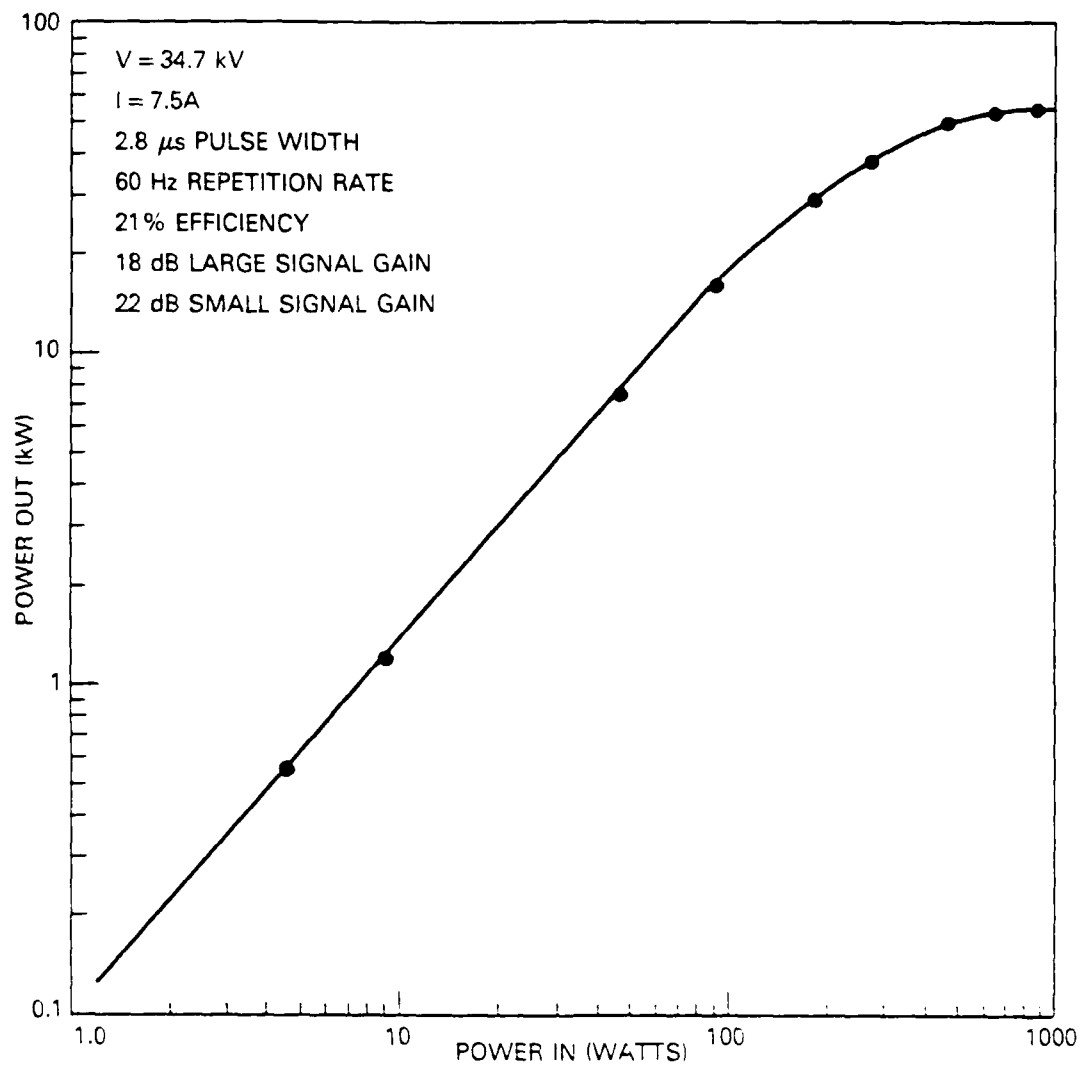


Figure 4. Drive Curve. Experimental drive curve showing largest peak power to date. The magnetic field is tapered and all cavities tuned to obtain maximum output power.

space-charge effects and, therefore, the velocity spread. Output microwave power increases, since the beam power is increasing faster than the efficiency drops with velocity spread. However, efficiency and gain decrease. The tapered magnetic profile which gave the best results increases from the gun until the end of the second cavity and then decreases. The magnetic field variation is approximately 32% from maximum to minimum field, as determined by the current in the magnetic field coils.

The bandwidth of the GKLY-101 device has also been examined. Figure 5 shows the calculated bandwidth with all cavities tuned to the same frequency and using the analysis of Reference 4. Our experiment has an α of approximately one, yielding a calculated bandwidth of 0.20%. Note that this calculation is for a uniform magnetic field and a beam current of 6 A. Experimentally, we observe (see Figure 6) a bandwidth (FWHM) of only 0.13%, although for a lower current, 3 A, the bandwidth increases to 0.26%. Further, the bandwidth can be increased to 0.43% by stagger tuning of the three cavities and tapering of the magnetic field. The stagger tuning is the dominant effect in broadening the bandwidth. The resolution of our measurement was limited to about 300 KHz (see Figure 7), which is approximately seven times the drive oscillator line width. This is due to the fact that the measurement is time-integrated, and over the entire pulse there is a large amount of FM noise. We believe the FM noise is related to voltage variations in the beam drive voltage. This is presently under investigation.

For our device, the bandwidth appears to be limited by the cavity Q values. For no stagger tuning, the limitation seems to be predominantly the drive cavity Q value. Since the first cavity has a Q of 600, the expected bandwidth (FWHM) is 0.2%. The limitation appears to be related to coupling the input signal into the first cavity. For staggered tuning, the limitation appears to be the output cavity Q of 235, which gives an expected bandwidth of 0.4%. Lower Q cavities should increase the bandwidth. Overall gain could be maintained by increasing the number of cavities.

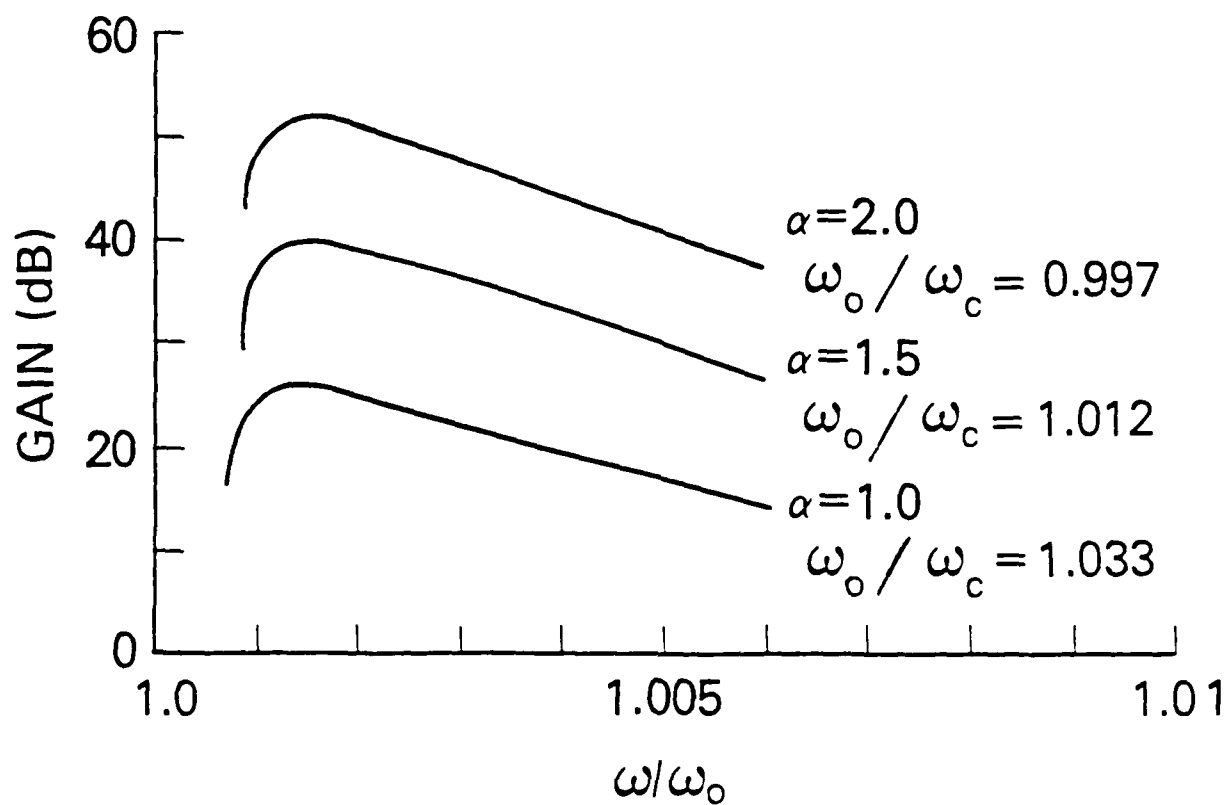


Figure 5. Theoretical Bandwidth Curve. Theoretical curves showing bandwidth for the GKLY-101 device at three values of α and ω_0 is the cavity resonant frequency and ω_c is the cyclotron frequency. For each value of α , ω_c has been adjusted for maximum gain.

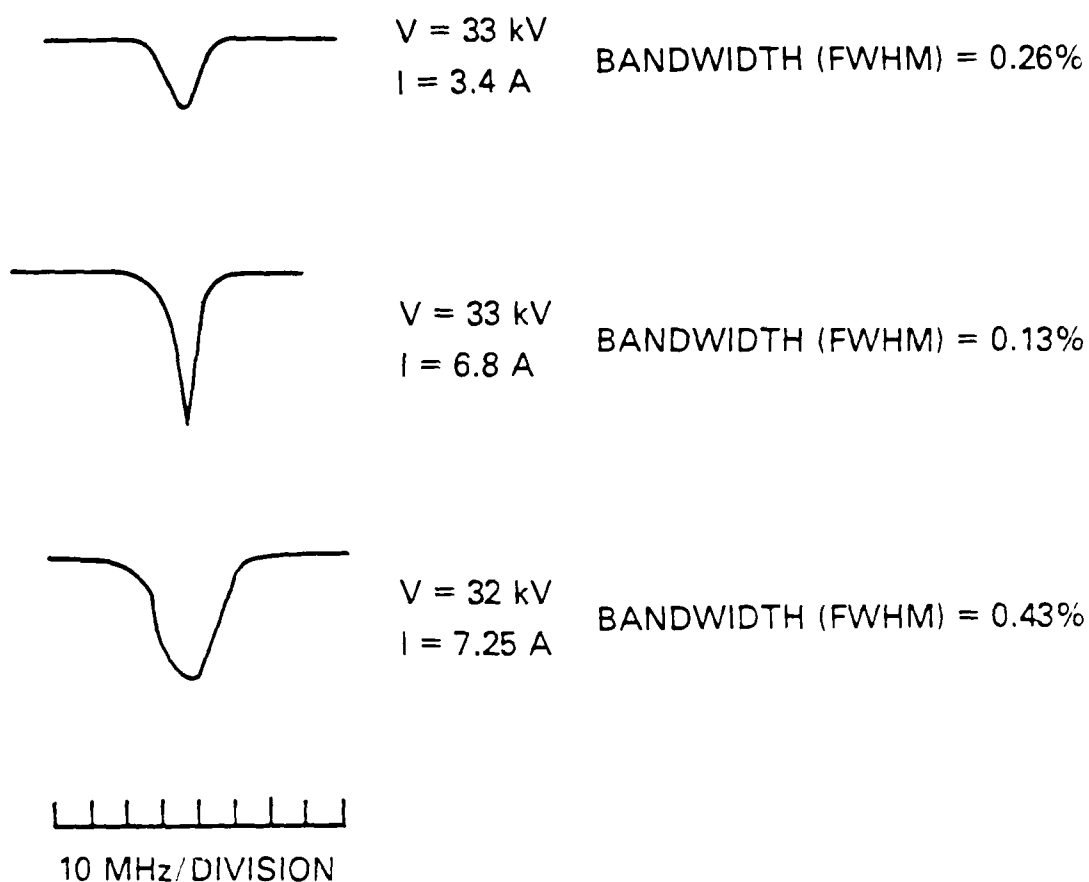


Figure 6. Experimental Measurements of Output Bandwidth. The upper two pictures show bandwidth measurements at two different beam currents. The lower picture shows the output bandwidth with staggered tuning and a tapered magnetic field.

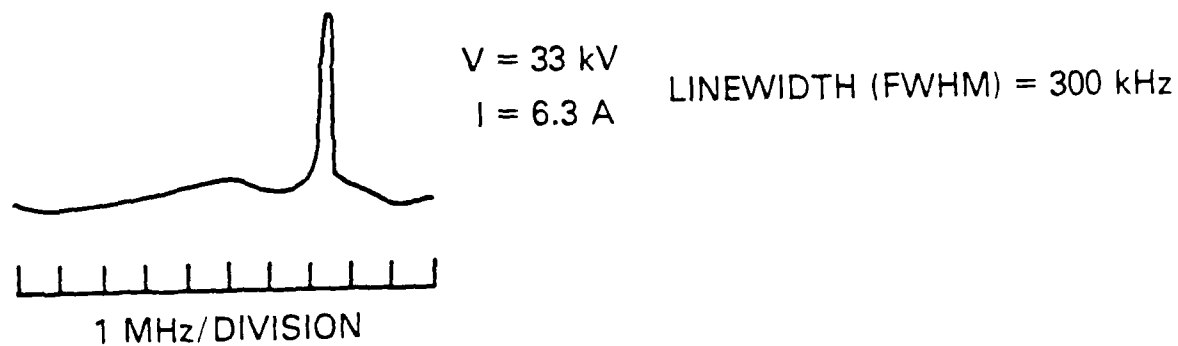


Figure 7. GKA Line Width. Shown is the gyrokystron line width for a single frequency drive signal. Broadening is due to FM noise.

Operation of the gyrokystron amplifier as a phase-locked oscillator is also being examined. This mode of operation has been predicted for the gyrokystron^{5,22} with a calculated drive curve as shown in Figure 8.²² The unique characteristic of this type of operation is the sharp transition from the linear amplifier region to the saturated locked-oscillator region. At the transition point a small increase in drive power will control the phase of a powerful oscillation. This phenomenon has been observed experimentally. The drive curve is shown in Figure 9 and, although performed at much lower power, shows the same qualitative features as the theoretical prediction. The power-locking ratio, $10 \log (P_{\text{oscc}}/P_{\text{drive}})$, is 56.5 dB at the transition. The phase-locked operation regime is achieved by tuning up an oscillation in the first cavity, then slightly detuning the magnetic fields near the gun so that the drive power can initiate the oscillation. The exact details of this type of operation are still under investigation. Without the input microwave drive signal, no output power is observed in the oscillator region. Apparently, the input microwave drive signal is lowering the threshold for oscillation in one of the three cavities, presumably by bunching of the electron beam. Preliminary observations of phase-locked oscillator operation suggest that the oscillations occur in the first cavity and are amplified in the following two cavities. It is therefore important that a high-power isolator, such as was used, be present in the input microwave drive line. For maximum utility as an actual tube, the oscillation will need to be excited in a cavity other than the input cavity to eliminate the large power emitted by the first cavity into the drive circuit. Recently, we have been able to adjust parameters to obtain oscillation only in the last cavity.²³

A phase correlation diagnostic was used to distinguish between a free oscillation and a phase-locked oscillation in the gyrokystron. The diagnostic compared the drive and output signals by giving a polar oscilloscope display, where the radial component of the display corresponded to the product of the amplitudes of the two signals and the angle from the x-axis, θ , of the polar display was the relative phase difference between the two signals. For a free oscillation, there is no phase relationship between the output and the drive signals. Therefore, the polar display of the diagnostic is a circle, while for

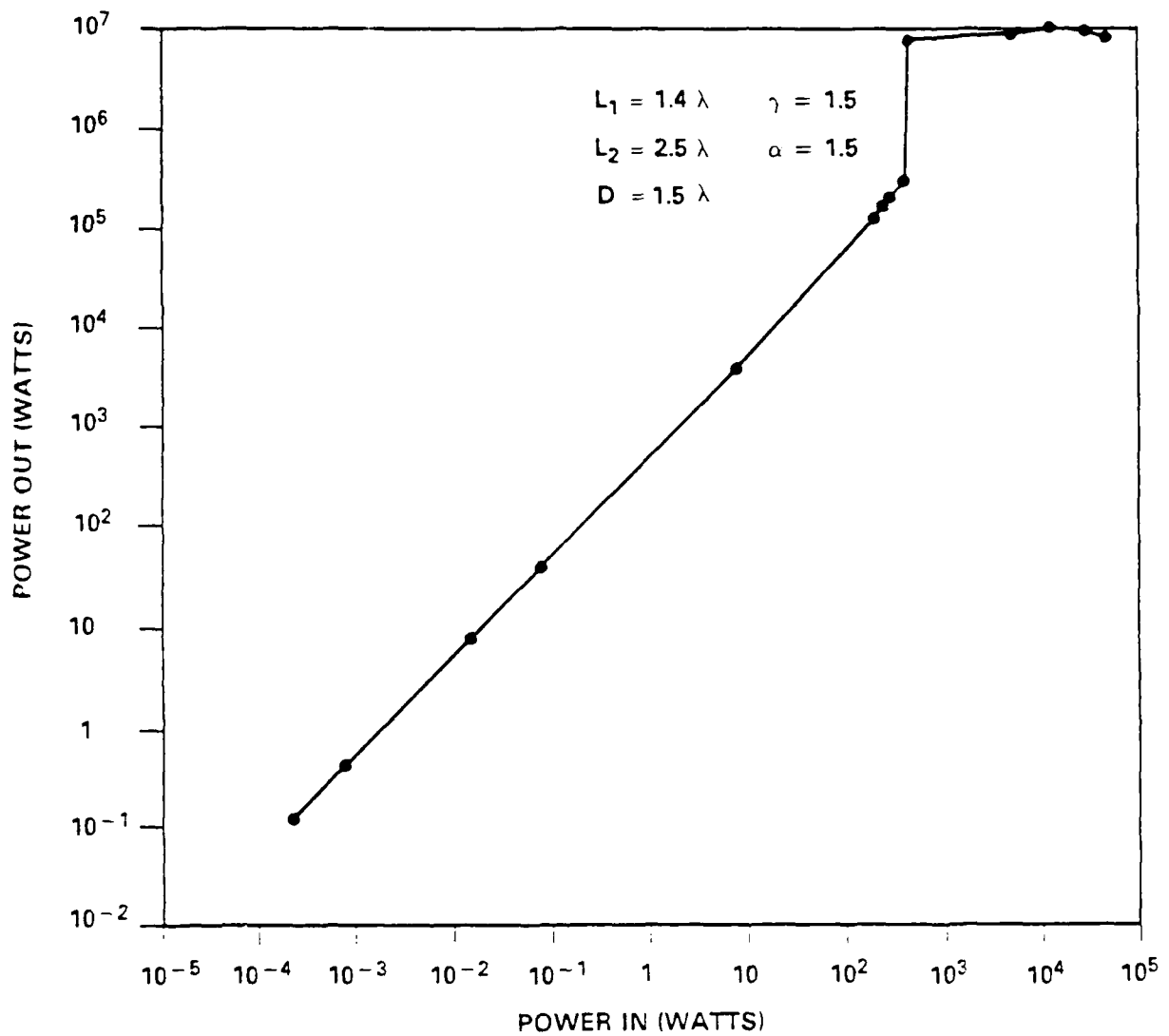


Figure 6. Theoretical Drive Curve for a Two-Cavity, Phase-Locked Gyrokystron Amplifier. L_1 and L_2 refer to the cavity lengths, D is the drift length between the two cavities, and γ is the relativistic factor.

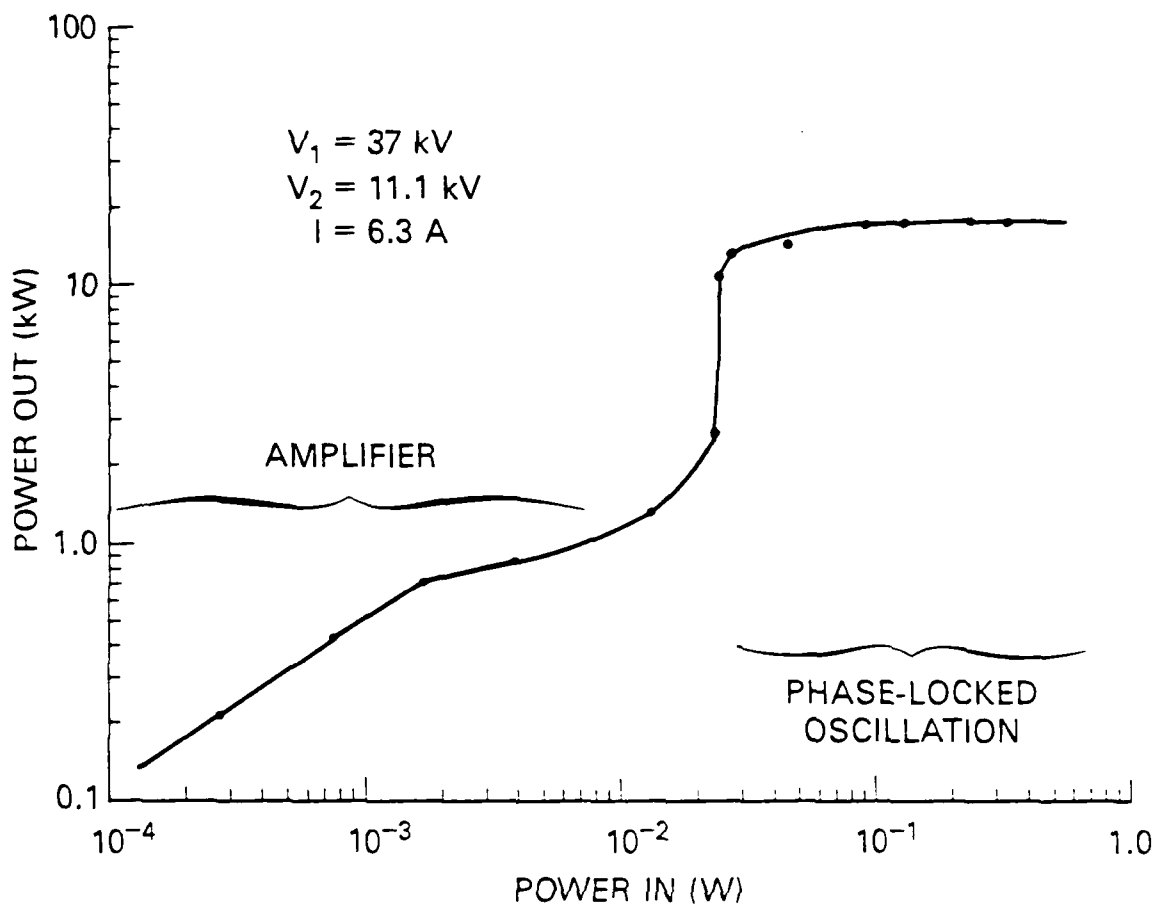


Figure 9. Experimental Drive Curve for GKLY-101 Phase-Locked Oscillator Operation.

phase-locked operation, the signals are related and a stationary point results for the display. The phase-locking behavior was confirmed by shifting the phase of the drive signal and verifying that the relative phase, ψ , remained constant.

Figure 10 shows data taken during operation in the locked-oscillator mode. Picture (a) shows the crystal detected output power in the sharp transition region of Figure 9. The two traces result from small fluctuations causing the output to jump from one side of the transition to the other. (When the device is operated at similar powers under amplifier conditions, no such jump is observed.) Picture (b) shows the output signal in the saturated region of the drive curve, and (c) is the corresponding phase diagnostic data showing phase-locked behavior. The explanation for phase control over the large output oscillation is that the oscillation in the first cavity is small and can be controlled by a small drive signal. This signal is then amplified in the following cavities.

We plan to continue the phase-locked oscillator work. In addition, the amplifier noise (AM and FM) is under examination.²⁴ The main new thrust, however, is in the design of a new amplifier tube. This GKA will have an overmoded circular output cavity, as will be required for high power operation. Initially, we are considering a circular TE_{121} output cavity. Operation will still be at the fundamental cyclotron frequency, and the drift tubes will be cut off to this frequency. Tuning and output power extraction techniques are presently under investigation. Plans for the development of a gun with a larger α are also underway.

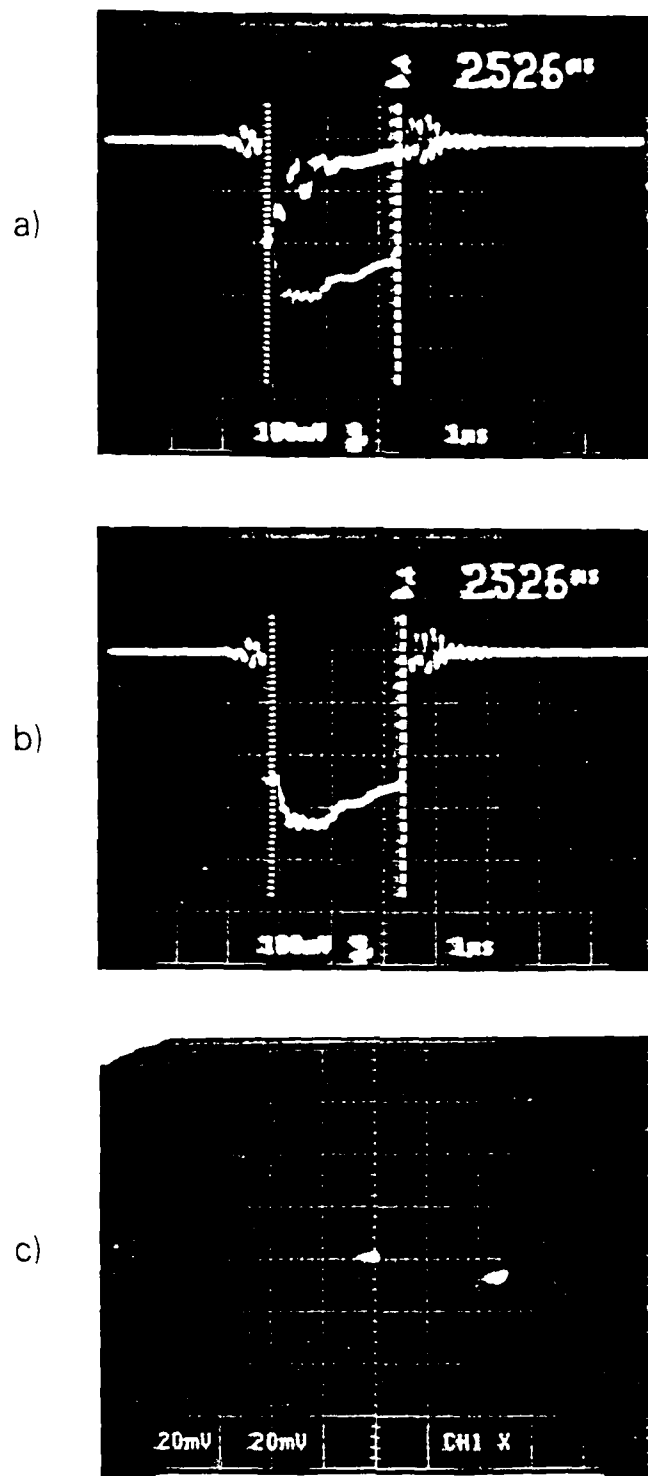


Figure 10. Phase-Locked Oscillator Performance. (a) Gyrokystron output at the transition, (b) Saturated output signal, and (c) Phase diagnostic showing phase locking in the saturated region.

SECTION 5

CONCLUSIONS

It has been shown that a gyrokylystron device can be stably operated. Further, reasonably large efficiencies ($\approx 30\%$) are possible. A 30% efficiency for our device corresponds to a perpendicular efficiency of 60%, which approaches the large values predicted in the Russian literature.^{13,14} This implies overall efficiencies of 50% are attainable for beams with $\alpha \approx 2$. Large signal gains of 20 dB at high power seems practical with a three-cavity device. Further, bandwidths seem to be restricted in the present geometry to about 0.4%; however, lower Q cavities would probably increase this bandwidth. Locked-oscillator performance has been observed. Theoretical predictions suggest that such devices are capable of larger output powers and efficiencies than amplifiers. We conclude that a gyrokylystron amplifier (or locked oscillator) presents an attractive choice for a high-power, high-efficiency, narrow-bandwidth microwave or millimeter wave device.

SECTION 6
ACKNOWLEDGMENTS

We wish to acknowledge the technical assistance of Frank Wood and Stan Swiadek in the design and assembly of the gyrokystron tube. This work was supported under a contract with the Office of Naval Technology.

SECTION 7

REFERENCES

1. B. Afrin and A. K. Ganguly, "A Three-Cavity Gyroklystron Amplifier Experiment," Int. J. Electron, 53, p. 709 (1982).
2. W. M. Bollen, A. K. Ganguly, B. Arfin, C. Sedlak and R. K. Parker, "Performance of a Three-Cavity Gyroklystron," Proceedings of the IEDM Digest, p 838 (1984).
3. A. K. Ganguly and K. R. Chu, "Analysis of Two-Cavity Gyroklystrons," Int. J. Electron., 51, p. 503 (1981).
4. A. K. Ganguly, A. W. Fliflet, and A. H. McCurdy, IEEE Transaction on Plasma Science, PS-13, p. 409, (1985).
5. R. S. Symons and J. R. Jory, "Cyclotron Resonance Devices," In Adv. Electron. Elec. Phys., 55, p. 1, Academic Press, NY (1981).
6. H. R. Jory, F. Friedlander, S. J. Hegji, J. F. Shively, and R. S. Symons, IEDM Digest, p. 234, (1979).
7. A. Andronov, V. A. Flayagin, A. V. Gaponov, L. Gol'denberg, M. I. Petelin, V. G. Usov, and V. K. Yulpatov, Infrared Phys., 18, p. 385, (1978).
8. J. M. Wachtel and J. L. Hirshfield, "Interference Beats in Pulse Stimulated Cyclotron Radiation," Phys. Rev. Lett., 17, p. 348, (1966).
9. H. R. Jory, F. Freidlander, S. J. Hegji, J. R. Shively, and R. S. Symons, "Gyrotrons for High-Power Millimeter Wave Generation," IEDM Digest, p. 234 (1977).
10. H. R. Jory, "Millimeter Wave Gyrotron Development Phase I," Technical Report RADC-TR-77-210 (1977).
11. S. J. Hegji and H. R. Jory, "High-Power Millimeter Wave Amplifier," Interim Report RADC-TR-78-235 (1978).
12. E. M. Demidovich, I. S. Kovalev, A. A. Kurayev, and F. G. Shevchenko, "Efficiency-Optimized Output Cavity Profiles that Provide a Higher Margin of Gyroklystron Stability," Radio Eng. Electron Phys., 19, No. 5, p. 96 (1974).
13. S. V. Kolosov and A. A. Kurayev, "Comparative Analysis of the Interaction at the First and Second Harmonics of the Cyclotron Frequency in Gyroresonance Devices," Radio Eng. Electron. Phys., 19, No. 10, p. 65 (1974).
14. A. A. Kurayev, F. G. Shevchenko, V. P. Shetakovich, "Efficiency-Optimized Output Cavity Profiles that Provide a Higher Margin of Gyroklystron Stability," Radio Eng. Electron Phys., 19, No. 10, p. 65 (1974).
15. V. I. Kavavets and O. I. Klimov, "The Electron Efficiency of a Monotron and Klystron with a Relativistic Polyhelical Electron Beam," Radio Eng. Electron Phys., 21, No. 11, p. 78 (1976).

16. R. S. Symons and H. R. Jory, "Small-Signal Theory of Gyrotrons and Gyroklystrons," Proceed. 7th Sympos. Eng. Probl. Fusion Res., p. 1111 (1976).
17. H. R. Jory and A. W. Trivelpiece, "Charged Particle Motion in Large Amplitude Electromagnetic Fields," Appl. Phys., 39, p. 3053 (1968).
18. I. S. Kovalev, A. A. Kurayev, S. V. Kolosov, and G. Yu. Slepian, "The Effect of Space Charge in Gyroresonance Devices with Thin Equally Mixed and Axially Symmetrical Electron Beams," Radio Tekh. Electron., 19, No. 5, p. 1112 (1974).
19. A. A. Kurayev and A. F. Stekol'nikov, "Study of Influence of Space-Charge Forces on Electron Bunching in Drift Tube of Gyroklystron," Radio Eng. Electron. Phys., 25, No. 9, p. 78 (1980).
20. A. P. Keier, "Electron Flux Bunching with Spread in Electron Velocities in A Gyroklystron with a Nonuniform Magnetic Field," Radio Phys. Quantum Elect., 21, No. 6, p. 631 (1978).
21. A. P. Keier, "Modes of Operation of Output Cavity of a Gyroklystron with Electron Velocity Spread and Nonuniform Magnetostatic Field," Radio Phys. Quantum Electron., 21, No. 6, p. 636 (1978).
22. W. M. Bollen, A. K. Ganguly, B. Arfin, M. Nagurney, and F. N. Wood, "Large Signal Analysis for High-Power Gyroklystron Amplifiers," presented at the 1984 IEEE Plasma Sciences Meeting in St. Louis.
23. A. H. McCurdy, C. M. Armstrong, and W. M. Bollen, "Gyrotron Phase Locking Using a Modulated Electron Beam," submitted to the 1986 IEEE Plasma Sciences Meeting in Saskatoon, Canada.
24. J. McAdoo, W. M. Bollen, V. L. Granastein, R. K. Parker, R. Smith, G. Thomas, and A. McCurdy, IEEE Trans. Nucl. Science, NS-32, p. 2963 (1985).

END

3-87

DTIC